ULTRASONIC-ASSISTED ELECTRODEPOSITION OF SnNi(C) COMPOSITE COATINGS

Katya Ignatova, Daniela Lilova

University of Chemical Technology and Metallurgy
Faculty of Chemical Technologies
Department of Inorganic and Electrochemical Productions
8 Kliment Ohridsky Blvd., Sofia 1797, Bulgaria
katya59ignatova@gmail.com (K.I.); dlilova@uctm.edu (D.L.)

Received 08 October 2024
Accepted 16 May 2025
DOI: 10.59957/jctm.v60.i5.2025.14

ABSTRACT

By changing various parameters: content of graphite particles, ultrasonic stirring and electrolyte temperature data on the growth rate, elemental composition and morphology of electrodeposited Sn-Ni(C) composites on copper were obtained. The coatings deposition was performed at galvanostatic conditions in gluconate-glycinate electrolyte with pH = 4 - 4.5. Fine graphite powder with concentrations of 1 - 4 g L^{-1} was added to the solution. Coatings deposited under "quiet" conditions are coarse-crystalline and the graphite particles are unevenly distributed. By increasing the temperature to 60°C, ultrasonic stirring and graphite content in the solution of 3 g L^{-1}, the coatings become finer-crystalline and smooth. The Ni content increased by about 11 wt. % and mова на Sn varies between 44 wt. % to 71 wt. % in these conditions. When applying ultrasonic stirring and when the graphite content in the solution increases from 0 to 4 g L^{-1}, the average growth rate of the coating varies around higher limits (from 108 mg cm^{-2} h^{-1} to 74 mg cm^{-2} h^{-1}) compared to " the "quiet" conditions (from 95 mg h^{-1} to 44 mg cm^{-2} h^{-1}).

Keywords: electrodeposition, graphite particles (C), composite coating, SnNi(C), ultrasonic stirring.

INTRODUCTION

Because of their attractive appearance, high hardness, corrosion and friction resistance, the dense Ni-based coatings are of interest to automobile and petroleum industries, machine-building and electronics [1 - 4]. Thanks to their magnetic properties, Ni-based coatings are very intensively studied and applied in sensors for hard disks, biosensors, microelectromechanical systems (MEMS) and electrotechnics [5 - 8].

Over the last 20 years, the interest in alloys based on transition metals has increased due to their attractive prices and excellent electrocatalytic properties towards hydrogen and oxygen electrode reactions (HER and OER resp.) in water electrolysis [4, 12, 13] and for HER in chlorine-alkaline electrolysis [14]. In the last decade, Sn-based alloys with transition elements (mainly nickel and cobalt) have been applied with increasing success as anodic materials in lithium-ion batteries (LIBs) [15 - 20] and sodium-ions batteries (NaIBs) [20, 21] because of the high theoretical capacitance of Sn (994 mAh g^{-1} for Sn compared to 372 mAh g^{-1} for graphite). Introducing of graphite, graphene and other particles in Sn-based anodic materials increases the current capacity and extends the battery life [4, 22].

To receive composite coatings with high quality and homogenous distribution of dispersed in solution and in the coating material, using the proper way to stir and deagglomerate the inert particles is important. An appropriate technique is electrodeposition with ultrasound assistance [23, 27]. The principles of action and theoretical aspects of the effect of the ultrasound stirring on the electrodeposition of metals and particles, using pure solutions and suspensions are presented in [23 - 27]. A million bubbles produced inside the solution at a high sound frequency cause the stirring effect realized by an

ultrasonic bath. Data on the application of ultrasound in the deposition of Ni and Ni-based alloys [28, 29] and of Ni(Al_2O_3) [30], Ni/SiC [31], Ni(Diamond) [9] composites are presented in the literature.

Some of the well-known compositions for electrodeposition of SnNi alloys are glycinate electrolyte [16], fluoride-chloride electrolyte [32], and alkaline pyrophosphate-chloride electrolyte with gelatin addition [33]. The glycinate electrolyte has the composition: 0.175 ÷ 0.068M $SnCl_2$, 1.262M $NiCl_2$, 0.5M $K_4P_2O_7$, 0.125 M glycine, 5 ml L^{-1} NH_3. In our previous work, the effect of the separate and co-presence of sodium gluconate and glycine on the deposition kinetics and morphology of SnNi alloy coating was investigated [34]. It has been found that glycine whit a concentration above 5 - 8 g L^{-1} gives coatings with better adhesion.

This study aimed to investigate the influence of ultrasonic stirring, the content of the graphite particles in the solution and its temperature on the particle distribution in coatings, elemental composition and morphology of SnNi(C) composite coatings.

EXPERIMENTAL

Composition of the electrolyte

The electrolyte for galvanostatic deposition of coatings on copper electrodes has the following composition: 95 g L^{-1} $SnCl_2 \times 5H_2O$ (0.42 M); 200 g L^{-1} $NiCl_2 \times 5H_2O$ (0.42 M); 100 g L^{-1} $C_6H_{11}NaO_7$ (sodium gluconate); addition of 100 g L^{-1} $C_2H_5NO_2$ (glycine); pH = 4 - 4.5. The high concentration of sodium gluconate and glycine provides the deposition of denser coatings. Fine graphite powder, based on soft carbon (type Soft) with concentrations of 1 - 4 g L^{-1} was added to the solution. The graphite powder used is distinguished by parallel arranged graphene layers with a high degree of defects, an average particle size of 3 - 8 μm, and is suitable for use in lithium-ion batteries [35]. The electrolyte is subjected to ultrasonic stirring both during the electrodeposition of the coating and 15 - 20 min before it for deagglomeration and good distribution of the graphite particles. A peculiarity of the preparation of the solutions is that the Sn salt was added to pre-dissolved sodium gluconate and glycine at a temperature of 50 - 60°C. The Ni salt, dissolved previously in distilled water, was added to the so-prepared stable solution. The pH value was adjusted to 4 - 4.5 using NaOH and HCl.

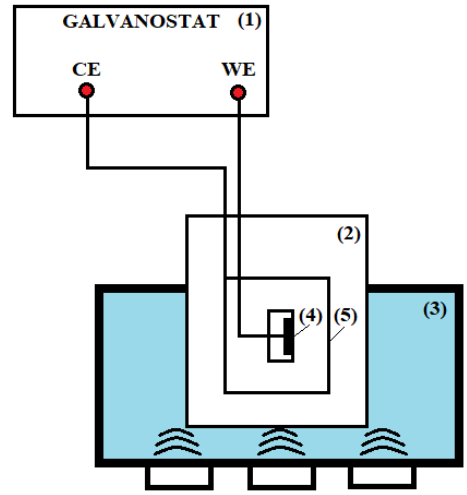

Fig. 1. Experimental schema of coating deposition: (1) galvanostat; (2) electrochemical cell; (3) ultrasonic bath; (4) copper working electrode (WE); (5) platinum counter electrode (CE).

Electrodeposition of the coatings

Fig. 1 shows a scheme of the experimental technique used in the study. A two-electrode cell contains a working copper electrode (WE) with a surface area of 4 cm^2 (2 cm / 2 cm) and a counter platinum electrode (CE) with an area of 20 cm^2. The cell was immersed in the thermostatic ultrasonic bath, Digital Ultrasonic Cleaner CD-4830 with volume 3 L and 36 kHz frequency.

The deposition was carried out under galvanostatic conditions using Galvanostat/Poten-tiostat OH-405 (Hungary) (1). All coatings were deposited at current density j = 7.5 mA cm^{-2}.

Pretreatment of the electrodes

Copper foil was used to prepare working electrodes; non-worked side was isolated. Before each experiment, the electrodes were subjected to pretreatment operations to clean possible contaminants and oxides on their surface: degreasing in an alcohol-ether mixture, washing in hot distilled water (80°C), glossy etching in a mixture of concentrated acids (HNO_3 : H_2SO_4 = 2 : 1) with an addition of 10 mL c. HCl in 100 mL of solution and subsequently rinsing with distilled water repeatedly. The platinum counter electrode was periodically left submerged for 5 - 10 min in a solution of 50 % HNO_3 heated to 50°C. After the deposition, the coated

electrodes were rinsed with distilled water and dried with filter paper.

Morphological and elemental analysis

The surface morphology of the samples was analysed by Scanning Electron Microscopy (SEM) using an SEM/FIB LYRA I XMU microscope of the company TESCAN with tungsten heated filament as an electronic source, 3.5 nm resolution at 30 kV and accelerating voltage from 200 V up to 30 kV. The microscope was equipped with an EDS detector, Quantax 200, company BRUKER for quantitative analysis. Spectroscopic resolution of the ED spectrometer of 126 eV was measured by the FWHM resolution of the Mn-Kα X-ray peak at 5.9 keV.

RESULTS AND DISCUSSION

Elemental composition

By varying various parameters: application of ultrasonic stirring with a frequency of 36 κHz, electrolyte temperature in the range of 20 - 60°C and graphite concentration 0 - 4 g L^{-1}, data about the elemental composition (Table 1) and the morphology of SnNi(C) coatings were obtained. To obtain more detailed information on the distribution of graphite particles in the coatings, elemental composition data were received at two different points on the surface of samples "1" and "5" (Table 1, Fig. 2 and Fig. 3). The two samples were deposited under different conditions: sample „1" - at 20°C, without ultrasonic stirring and low graphite content of 1 g L^{-1} and sample „5" - at 60°C, with ultrasonic stirring and graphite content of 3 g L^{-1}.

As can be seen from Table 1, in the absence of ultrasonic stirring and with a graphite content of 1 g L^{-1}, the temperature rising from 20 to 40°C results in a slight change in the coating composition - only 2 - 3 % for Sn and less than 1 % for Ni and oxygen (Table 1, sample "1" - Point 2 and sample "2").

EDS analysis shows that the oxygen content in the places of incorporated graphite particles is about 20 wt.% higher than in the other areas - 35.97 wt. % for point 1 and 15 wt. % for point 2 in sample "1" (Table 1, Fig. 2). In the same place, the Sn content, although decreasing, remains high (43.95 wt. %). In the regions outside the embedded graphite particles, with increasing temperature from 40°C to 60°C and simultaneous application of ultrasound under constant other conditions, the Ni content increases from 12.62 wt. % to 23.24 wt. % in sample "5" (Table 1, Fig. 3). In the areas of embedded graphite particles, it is 5.5 wt. % (Fig. 3, point 1 for sample "5"). Under the same conditions, a decrease in the oxygen content of the coatings was found.

SEM images of samples "1" and "5", shown in Fig. 2 and Fig. 3, clearly illustrate the differences in morphology as the deposition conditions change. Sample "1", received at low temperature and without ultrasound, has a rougher structure (Fig. 2). Sample "5", obtained by ultrasonic stirring of the solution, high temperature (60°C), and at a graphite content of 3 g L^{-1}, has a fine-crystalline structure (Fig. 3). This is mainly due to the

Table 1. Elemental composition of SnNi(C) coatings, deposited under the relevant set of conditions: ultrasonic stirring (US), electrolyte temperature (t, °C), content of graphite particles in the solution in g L^{-1}.

Sample	US	t, °C	Graphite, g L^{-1}	Sn, wt.%	Ni, wt.%	C, wt.%	O, wt.%
1, Point1	-	20	1	43.95	4.91	15.18	35.97
1, Point 2	-	20	1	66.84	14.65	5.15	13.37
2	-	40	1	69.01	14.24	3.78	12.97
3	+	40	1	71.45	12.07	3.92	13.10
4	+	40	2	70.06	12.62	4.32	13.15
5, Point 1	+	60	2	16.89	5.50	54.97	22.64
5, Point 2	+	60	2	66.21	23.24	3.38	7.17
6	+	60	3	58.23	30.98	4.56	6.23
7	+	60	4	63.35	22.82	6.79	7.04

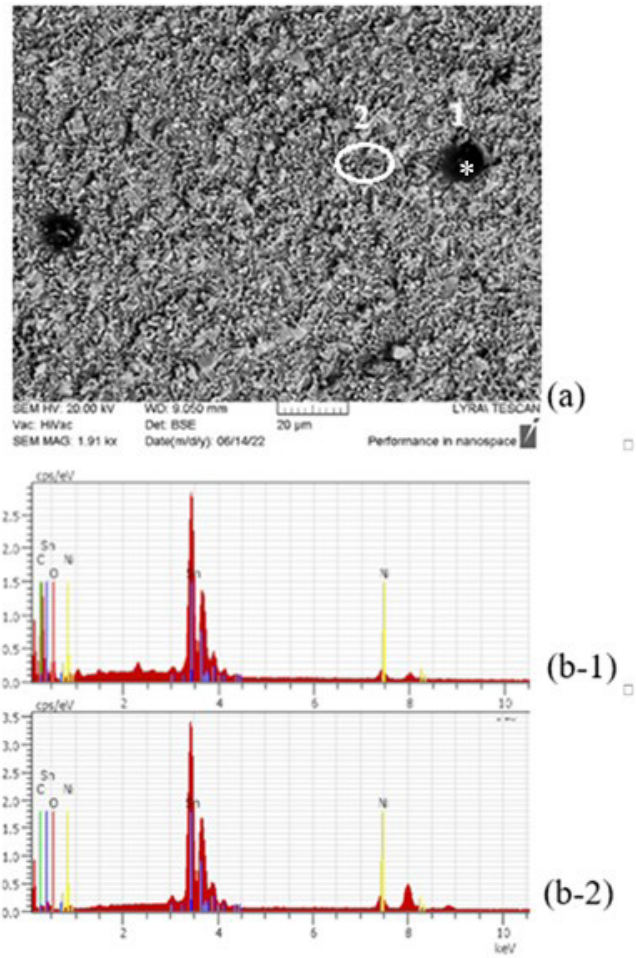

Fig. 2. SEM image and EDS spectrum in two points for sample "1" from Table 1.

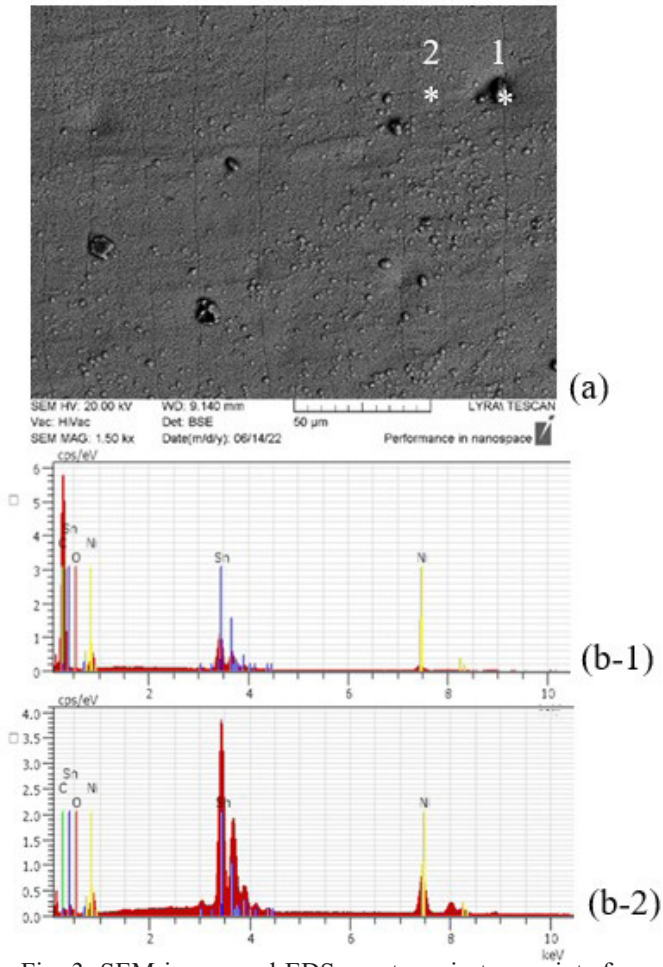

Fig. 3. SEM image and EDS spectrum in two points for sample "5" from Table 1.

nickel enrichment of the alloy. In these conditions, the nickel content reaches a maximum value of 30.98 wt. % (Table 1, sample "5"). It is assumed that the established change in the composition of the coating is due to a change in the hydrodynamics of the electrolyte under conditions of high temperature and simultaneous application of ultrasound. In these conditions, the deposition of the metal with greater kinetic difficulties, i.e., nickel, is facilitated [34].

Structure and morphology of coatings

The change in appearance of the coatings, deposited under different conditions, is shown in Fig. 4. All coatings are smooth and shiny and change color with increasing temperature, application of ultrasound and changing graphite content. The coating of pure Ni is grey, and those of the SnNi(C) coating, depending on the graphite content, goes from yellow (sample "2") to light grey (samples "5" and "6") and dark grey colour (sample "4"), all of which are smooth and shiny.

The SEM images in Fig. 5 show more clearly the change in the morphology of the coatings with varying deposition conditions. In the absence of ultrasonic stirring at a low temperature (20 °C) and a graphite content of 1 g L^{-1}, the coatings are coarse-crystalline, and the graphite particles are unevenly distributed (Fig. 5 a-a**).

Increasing the temperature in the solution up to 40°C without ultrasonic stirring at the same graphite content in the solution of 1 g L^{-1} does not cause a change in the structure of the coatings but affects the graphite distribution, which is more uniform (Fig. 5 b-b**). When applying ultrasonic stirring under the same other conditions, the coatings acquire a fine crystalline

Fig. 4. Photographic images of coatings of Ni (the first photo) and of SnNi(C) on copper electrode (samples "2", „5", „6" and „7" from Table 1).

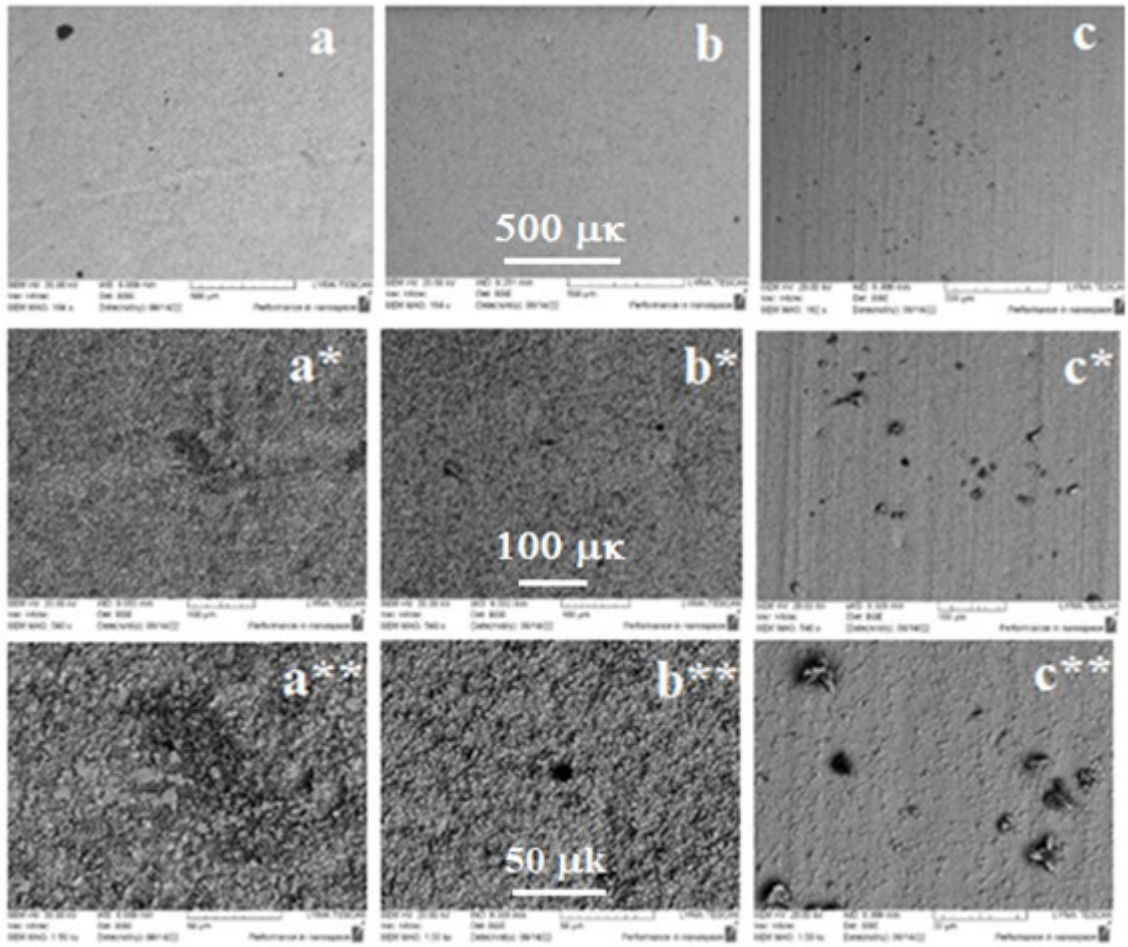

Fig. 5. Effect of the temperature and ultrasonic treatment at graphite content in the solution of 1 g L^{-1}: SEM images of SnNi(C) coatings - samples "1" (a-a**); "2" (b-b**); "3" (c-c**) from Table 1.

structure and are smooth at the base and the graphite particles are more uniformly distributed (Fig. 5 c-c**). The average diameter of graphite agglomerates is about 8 - 18 μm. It is seen that only ultrasound-assisted electrodeposition (all other conditions being identical) gives a smooth SnNi(C) composite coating with very uniform distribution of graphite particles on the surface. The composition of the coating, according to EDS data, corresponds to Ni(C) alloy with included oxides.

The effect of increasing graphite concentration in the electrolyte from 3 to 4 g L^{-1} at the temperature of 60°C and ultrasonic stirring of the electrolyte on the morphology of the composite SnNi(C) coatings was studied. Fig. 6 shows SEM images of the coatings at three

different magnifications. The comparison of the images from Fig. 6 c-c** to those from Fig. 6 a-a** for samples "1" and "5" resp. shows that the higher temperature and increase the graphite content in the solution up to 3 g L^{-1} have a favourable effect on the morphology of the coatings. The structure becomes more fine-crystalline and the distribution of the graphite particles on the coating surface is uniform in these conditions. When the graphite concentration is further increased to 4 g L^{-1}, a rather uneven distribution of graphite agglomerations on the surface is obtained (Fig. 6 b-b**). It can be assumed that the critical concentration of the graphite is 3 g L^{-1}. Increasing the graphite concentration in the solution above this critical concentration would be ineffective if a composite coating with a uniform graphite distribution is required.

Growth rate of the coating mass

The growth rate (GR) of the coating mass is estimated by the Eq. (1):

$$GR = m_2 - m_1 = \Delta m/S.t_{el}, mg\,cm^{-2}h^{-1} \quad (1)$$

where m_1 [mg] is the mass of the electrode before

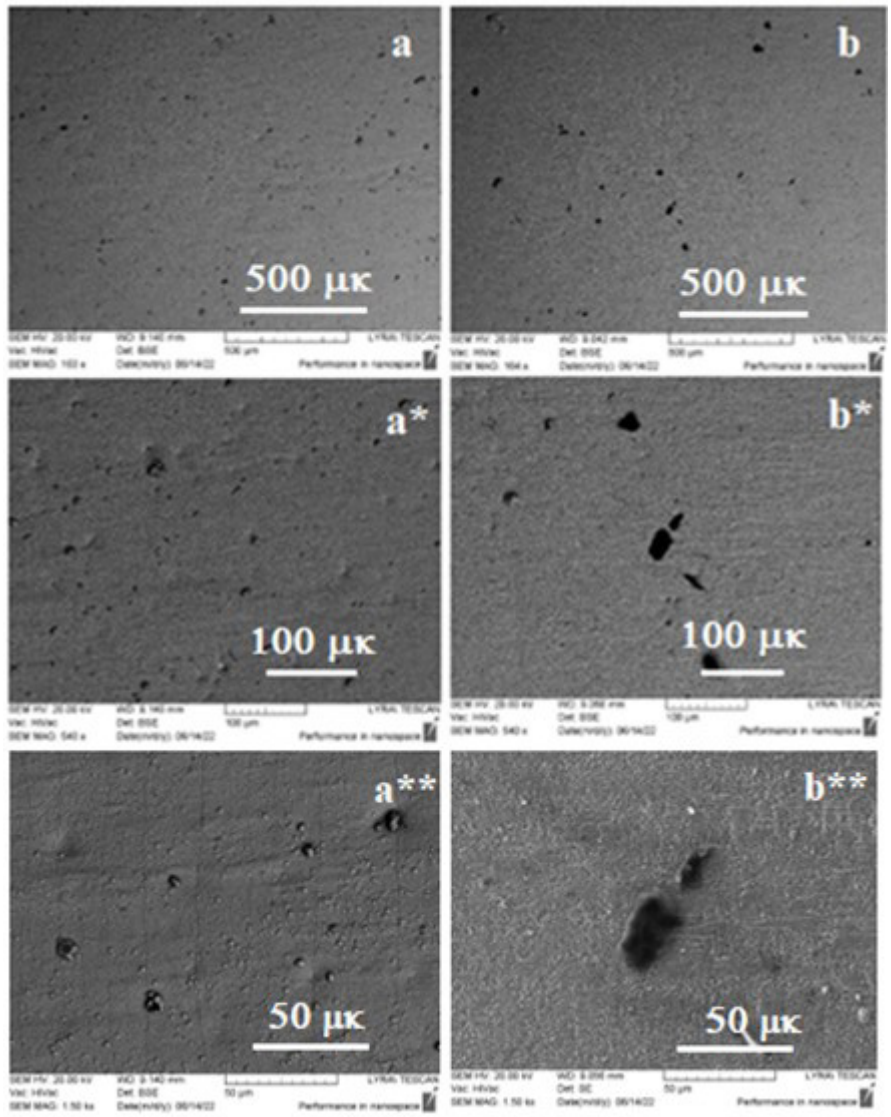

Fig. 6. Influence of the graphite content in the solution on the structure of the coatings: SEM images of samples "5" and "7" from Table 1 at three different magnifications.

electrolysis, m_2 [mg] - the mass of the electrode after electrolysis, S - electrode surface [cm^2] and t_{el} [h] is the time for which the electrolysis itself is carried out.

Fig. 7 shows the variation of the mass growth of the coatings depending on the concentration of graphite in the solution and the application of ultrasound. The dependences show that when applying ultrasonic stirring, the increase in the mass of the coating occurs at a higher rate (Fig. 7, curve 1) compared to that under "quiet" conditions (Fig. 7, curve 2).

The growth rate of the coating mass decreased with increasing graphite concentration in the solution regardless of the application of ultrasonic stirring. It is changed from 108 mg cm^{-2} h^{-1} to 74 mg cm^{-2} h^{-1} at ultrasonic stirring (Fig. 7, curve 1) and from 95 mg cm^{-2} h^{-1} to 44 mg cm^{-2} h^{-1} under "quiet" conditions (Fig. 7, curve 2) with increasing of graphite concentration in the solution from 0 to 4 g L^{-1}. The obtained data can be explained by the fact that the ultrasonic stirring of the solution affects the thickness of the formed diffusion layer, which becomes thinner and therefore increases the limiting current density, leading to a higher coating deposition rate. Increasing the concentration of graphite particles in an aqueous suspension leads to a decrease in the electrical conductivity of the solution, which hinders the movement of ions by migration and therefore reduces the deposition rate.

CONCLUSIONS

The following conclusions can be drawn from the presented research: i/ Elemental composition, morphology and mass growth rate of SnNi(C) alloy composites were investigated in galvanostatic mode depending on the ultrasonic stirring of the solution, temperature and concentration of graphite particles; ii/ The coatings deposited under "quite" conditions were found to be coarse-crystalline and the graphite particles were unevenly distributed within; iii/ The optimal graphite concentration in the solution, in which a uniform graphite particles distribution in the coatings is formed at the conditions of ultrasonic stirring and a temperature of 60 °C, is from 1 to 3 g L^{-1}; iv/ As the concentration of graphite in the solution increases from 0 to 4 g L^{-1} the growth rate of the coating mass decreases from 108 mg cm^{-2} h^{-1} to 74 mg cm^{-2} h^{-1} under ultrasonic stirring and from 95 mg cm^{-2} h^{-1} to 44 mg cm^{-2} h^{-1} under "quiet" conditions.

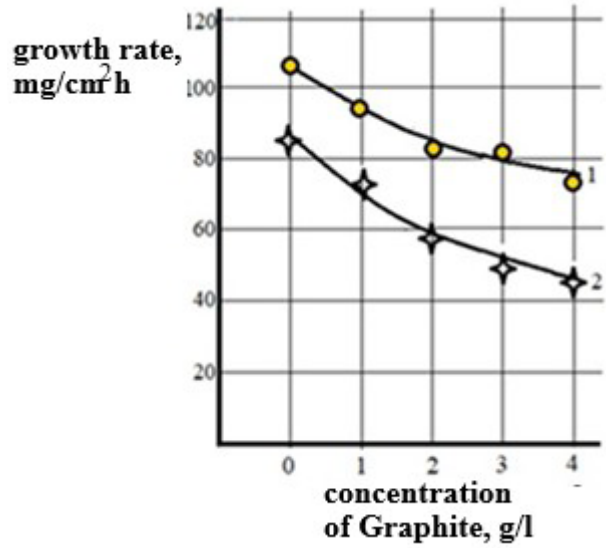

Fig. 7. The growth rate of SnNi(C) coating mass (GR, mg cm^{-2} h^{-1}) depending on the concentration of graphite in the solution (g L^{-1}) and application of ultrasound: Curve 1 - under ultrasound stirring; Curve 2 - under "quiet" conditions.

Acknowledgements

The authors are grateful to the Scientific Research Section of University of Chemical Technology and Metallurgy - Sofia for financial support via Projects No 12224 (2022) and No 12331 (2023).

***Authors' contributions**: K.I.: Conceptualization, Experimental work, Writing - Original draft and editing; D.L.: Experimental work, Data collecting, Review.*

REFERENCES

1. K.Y. Sasaki, B. Talbot, Electrodeposition of iron-Group metals and binary alloys from sulfate baths, J. Elecrochem.Soc., 145, 3, 1998, 981-990.
2. C. Ma, S.C. Wang, L.P. Wang, F.C. Walsh, R.J.K. Wood, The electrodeposition and characterisation of low-friction and wear-resistant Co-Ni-P coatings, Surf. Coating. Technol., 235, 2013, 495-505.
3. C. Ma, S.C. Wang, F.C. Walsh, The electrodeposition of nanocrystalline Cobalt-Nickel-Phosphorus alloy coatings: review, Trans. IME, Int. J. Surf. Eng. Coat., 93, 5, 2015, 275-282.
4. T.V. Vineesh, S. Mubarak, M.G. Hahm, V. Prabu, S.

Alwarapp, T.N. Narayanan, Controllably alloyed, low density, free-standing Ni-Co and Ni-Graphene sponges for electrocatalytic water splitting, Scientific Repotrts, 2016, 31202, doi: 101038/srep312026.
5. L. Peter, J. Padar, E. T.-Kadar, A. Cziraki, P. Soki, L. Pogany, I. Bakonyi, Electrodeposition of CoNiCu/Cu multilayers 1. Composition, structure and magnetotransport properties, Electrochim. Acta, 52, 2007, 3813-3821.
6. S. Armyanov, M. Maksimov,Structure, Internal stress and magnetic properties of electrodeposited Co-Ni alloys, IEEE Trans. Magn., 14, 5, 1978, 855-857.
7. G. Nabiyouni, W. Schwarzacher, Z. Rolik, I. Bakonyi, GMR and Magnetic Properties of electrodeposited CoNiCu/Cu multilayers, J. Magn. Mater, 253, 2002, 77-85.
8. D. Kim, D.-Y. Park, B.Y. Yoo, P.T.A. Sumodjo, N.V. Myung, Magnetic properties of nanocrystalline iron group thin film alloys electrodeposited from sulfate and chloride baths, Electrochim. Acta, 48, 2003, 819-830.
9. L. Baosong, M. Tianyong, Ch. Hongqiang, J. Wang, D.Shengsong, M. Yicheng, W. Zhang, Ultrasonic-assisted electrodeposition of Ni/diamond composite coatings and its structure and electrochemical properties, Ultrason. Sonochem., 73, 5, 2021, 105475.
10. M. Torabi, A. Dolati, A kinetic study on the electrodeposition of nickel nanostructure and its electrocatalytic activity for hydrogen evolution reaction, J. Appl.Electrochem., 40, 2010, 1941-1947.
11. I. Paseka, Hydrogen evolution reaction on amorphous Ni-P and Ni-S electrodes and the internal stress in a layer of these electrodes, Electrochim. Acta, 47, 6, 2001, 921-931.
12. R.K. Shervedani, A. Lasia, Studies of the hydrogen evolution reaction on Ni-P electrodes., J. Electrochem. Soc. 144, 2, 1997, 511-519.
13. J.J. Podesta, R.C.V. Piatti, A.J. Arvia, The influence of iridium, ruthenium and palladium on the electrochemical behaviour of Co-P and Ni-Co-P base amorphous alloys for water electrolysis in KOH aqueous solutions, Int. J. Hydrogen Energy, 20, 2, 1995, 111-122.
14. V.D. Jovic, U.C. Lacnjevac, B.M. Jovic, N.V. Krstalc, Electrodeposited, Ni-based, non-noble metal coatings as cathodes for hydrogen evolution in chlor-alkali electrolysis, Review paper, Zastita. Materijala, 55, 2, 2014, 111-125.
15. H. Zhang, T. Shi, P.V. Braun, 3D Scaffolded Nickel-Tin Li-Ion Anodes with Enhanced Cyclability, Adv. Mater., 28, 4, 2016, 742-749.
16. M. Uysal, H. Gormus, R. Karslioglu, A. Alp, H. Akbulut, Electrochemical performance of pulse electrodeposited Sn-Ni/MWCNT composite anode for Li-ion batteries, Proceedings of the 3rd international congress APMAS 2013, Acta Phys. Pol. A, 125, 2, 2014, 353-356.
17. K. Nishikawa, K. Dokko, K. Kinishita, S.W. Woo, K. Kanamura, Three-dimensionally ordered macroporous Ni-Sn anode for lithium batteries, J. Power Sources, 189, 2009, 726-729.
18. M. Lu, Y. Tian, Y. Li, B. Huang, Synthesis and Characterization of Spherical-Like Tin-Nickel Alloy as Anode for Lithium Ion Batteries, Int. J. Electrochem. Sci., 7, 1, 2012, 760-767.
19. X. L. Wang, W.Q. Han, J. Chen, J. Graetz, Single-Crystal Intermetallic M-Sn (M = Fe, Cu, Co, Ni) Nanospheres as Negative Electrodes for Lithium-Ion Batteries, ACS Appl. Mater. Interf., 2, 5, 2010, 1548-1551.
20. H. Ying, W.Q. Han, Metallic Sn-Based Anode Materials: Application in High-Performance Lithium-Ion and Sodium-Ion Batteries, Adv.Sci. (Weinh), 4, 11, 2017, 1-35.
21. Y. Yui, Y. Ono, M. Hayashi, Y. Nemoto, K. Hayashi, K. Asakura, and H. Kitabayashi, Sodium-Ion Insertion/Extraction Properties of Sn-Co Anodes and Na Pre-Doped Sn-Co Anodes, J. Electrochem. Soc., 162, 2, 2015, A3098-A3102.
22. V. Milanova, I. Markova, M. Piskin, T. Stankulov, T. Petrov, I. Denev, Synthesis and study of carbon-based nanocomposites with Co-Sn nanoparticles for electrode materials, J. Chem. Technol. Metall., 50, 3, 2015, 288-298.
23. I. Tudela, Y. Zhang, M. Pal, I. Kerr, A.J. Cobley, Ultrasound-assisted electrodeposition of composite coatings with particles, Surf. Coat. Techn., 259, C, 2014, 363-373.
24. A. Mallik, B.C. Ray, Evolution of principle and practice of electrodeposited thin film: a review on effect of temperature and sonication, Res. Int. J. Electrochem., 2011, Article ID 568023, 1-16.
25. B.G. Pollet, Editor, Power ultrasound in

electrochemistry: From versatile laboratory tool to engineering solution, John Wiley & Sons: Hoboken, NJ, USA, 2012.
26. B.G. Pollet, A novel method for preparing PEMFC electrodes by the ultrasonic and sonoelectrochemical techniques., Electrochem. Comm., 11, 2009, 1445-1448.
27. J.M. Costa, A.F.de Al.Neto, Ultrasound-assisted electrodeposition and synthesis of alloys and composite materials: A review, Ultras. Sonochem., 68, 2020, 105193.
28. K. Kobayasi, A. Chiba, N. Minami, Effects of ultrasound on both electrolytic and electroless nickel depositions, Ultrasonics, 38, 2000, 676-681.
29. S. Tan, H. Algül ̧ E. Kiliçaslan, Ah. Alp, H. Akbulut, M. Uysal, The effect of ultrasonic power on high temperature wear and corrosion resistance for Ni based alloy composite coatings, Colloids and Surf. A: Physicochem. and Eng. Aspects, Part A, 656, 1, 2023, 130345.
30. E. García-Lecina, I. García-Urrutia, J.A. Díez, J. Morgiel, P. Indyka, A comparative study of the effect of mechanical and ultrasound agitation on the properties of electrodeposited Ni/Al_2O_3 nanocomposite coatings, Surf. Coat. Technol., 206, 2012, 2998-3005.
31. G. Gyawali, S.H. Cho, D.J. Woo, S.W. Lee, Pulse electrodeposition and characterisation of Ni-SiC composite coatings in presence of ultrasound, Transactions, 90, 5, 2012, 274-281.
32. J.W. Cuthbertson, N. Parkinson, H.P. Rooksby, Electrodeposition of Tin-Nickel Alloy Plate from Chloride-Fluoride Electrolytes, J. Electrochem. Soc., 100, 3, 1953, 107-119.
33. P.R. Narayanan, S.V.S.N. Murty, Electrodeposition of Sn-Ni Alloy Coatings and their characterization, Adv. Mater. Manuf. Proc., 9, 2015, 655-658.
34. K. Ignatova, L. Vladimirova, Electrodeposition and morphology of SnNi powders in gluconate and fluoride-gluconate electrolyte in the presence of Glycin, Oxidation Communications, 45, 3, 2022, 538-545.
35. D. Saurel, J. Segalini, M. Jauregui, A. Pendashteh, B. Daffos, P. Simon, M. Casas-Cabanas, A SAXS outlook on disordered carbonaceous materials for electrochemicalenergy storage, Energy Storage Materials, 21, 5, 2019. https: //doi.org/10.1016/j.ensm.2019.05.007